2

Wireless Communications and Multitaper Analysis: Applications to Channel Modelling and Estimation

Sahar Javaher Haghighi and Serguei Primak
Department of Electrical and Computer Engineering,
The University of Western Ontario
London, Ontario, Canada

Valeri Kontorovich
CINVESTAV
Mexico

Ervin Sejdić
Bloorview Research Institute
Institute of Biomaterials and Biomedical Engineering
University of Toronto
Toronto, Ontario, Canada

1. Introduction

The goal of this Chapter is to review the applications of the Thomson Multitaper analysis (Percival and Walden; 1993b), (Thomson; 1982) for problems encountered in communications (Thomson; 1998; Stoica and Sundin; 1999). In particular we will focus on issues related to channel modelling, estimation and prediction.
Sum of Sinusoids (SoS) or Sum of Cisoids (SoC) simulators (Patzold; 2002; SCM Editors; 2006) are popular ways of building channel simulators both in SISO and MIMO case. However, this approach is not a very good option when features of communications systems such as prediction and estimation are to be simulated. Indeed, representation of signals as a sum of coherent components with large prediction horizon (Papoulis; 1991) leads to overly optimistic results. In this Chapter we develop an approach which allows one to avoid this difficulty. The proposed simulator combines a representation of the scattering environment advocated in (SCM Editors; 2006; Almers et al.; 2006; Molisch et al.; 2006; Asplund et al.; 2006; Molish; 2004) and the approach for a single cluster environment used in (Fechtel; 1993; Alcocer et al.; 2005; Kontorovich et al.; 2008) with some important modifications (Yip and Ng; 1997; Xiao et al.; 2005).
The problem of estimation and interpolation of a moderately fast fading Rayleigh/Rice channel is important in modern communications. The Wiener filter provides the optimum solution when the channel characteristics are known (van Trees; 2001). However, in real-life applications basis expansions such as Fourier bases and discrete prolate spheroidal sequences (DPSS) have been adopted for such problems (Zemen and Mecklenbräuker; 2005; Alcocer-Ochoa et al.; 2006). If the bases and the channel under investigation occupy the same band, accurate

and sparse representations of channels are usually obtained (Zemen and Mecklenbräuker; 2005). However, a larger number of bases is required to approximate the channel with the same accuracy when the bandwidth of the basis function is mismatched and larger than that of the signal. A bank of bases with different bandwidths can be used to resolve this particular problem (Zemen et al.; 2005). However, such a representation again ignores the fact that in some cases the band occupied by the channel is not necessarily centered around DC, but rather at some frequency different from zero. Hence, a larger number of bases is again needed for accurate and sparse representation. A need clearly exists for some type of overcomplete, redundant bases which accounts for a variety of scenarios. A recently proposed overcomplete set of bases called Modulated Discrete Prolate Spheroidal Sequences (MDPSS) (Sejdić et al.; 2008) resolves the aforementioned issues. The bases within the frame are obtained by modulation and variation of the bandwidth of DPSSs in such a way as to reflect various scattering scenarios.

2. Theoretical Background

2.1 Discrete Prolate Spheroidal Sequences

The technique used here was introduced first in (Thomson; 1982) and further discussed in (Percival and Walden; 1993b). We adopt notations used in the original paper (Thomson; 1982). Let $x(n)$ be a finite duration segment of a stationary process, $n = 0, \cdots, N-1$. It can be represented as

$$x(n) = \int_{-1/2}^{1/2} \exp\left(j2\pi f[n-(N-1)/2]\right) dZ(f) \tag{1}$$

according to the Cramer theorem (Papoulis; 1991). It is emphasized in (Thomson; 1982) that goal of the spectral analysis is to estimate moments of $Z(f)$, in particular its first and second moments from a finite sample $x(n)$. However, spectral analysis is often reduced only to considering the second centered moment

$$S(f)df = \mathcal{E}\left\{|dZ(f)|^2\right\} \tag{2}$$

well known as the spectrum (power spectral density). In the case of continuous spectrum the first moment of $dZ(f)$ is zero and it is usually not considered. However, in the case of a line or mixed spectrum one obtains

$$\mathcal{E}\left\{dZ(f)\right\} = \sum_k \mu_k \delta(f - f_k) df \tag{3}$$

where μ_k is the amplitude of the harmonic with frequency f_k.
The Discrete prolate spheroidal sequences (DPSS) are defined as solutions to the Toeplitz matrix eigenvalue problem (Thomson; 1982; Slepian; 1978)

$$\lambda_k(N,W)u_k(N,W;n) = \sum_{m=0}^{N-1} \frac{\sin\left(2W(n-m)\right)}{\pi(n-m)} u_k(N,W;m) \tag{4}$$

Their discrete Fourier transform (DFT) is known as Discrete Prolate Spheroidal Wave Functions (DPSWF) (Slepian; 1978)

$$U_k(N,W;f) = \sum_{n=0}^{N-1} u_k(N,W;n)\exp(-j2\pi nf) \tag{5}$$

In particular, if $f = 0$, equation (5) can be rewritten as

$$U_k(N,W;0) = U_k(0) = \sum_{n=0}^{N-1} u_k(N,W;n) \tag{6}$$

The DPSS are doubly orthogonal, that is, they are orthogonal on the infinite set $\{-\infty,...,\infty\}$ and orthonormal on the finite set $\{0,1,...,N-1\}$, that is,

$$\sum_{-\infty}^{\infty} v_i(n,N,W)v_j(n,N,W) = \lambda_i\delta_{ij} \tag{7}$$

$$\sum_{n=0}^{N-1} v_i(n,N,W)v_j(n,N,W) = \delta_{ij}, \tag{8}$$

where $i,j = 0,1,...,N-1$.
A number of spectral estimates, called eigen coefficients, are obtained using DPSS $u_k(N,W;n)$ as time-domain windows

$$Y_k(f) = \sum_{n=1}^{N-1} x(n)u_k(N,W;n)\exp(-j2\pi nf) \tag{9}$$

Since for a single line spectral component at $f = f_0$

$$\mathcal{E}\{Y_k(f)\} = \mu U_k(N,W;f-f_0) + \mu^* U_k(N,W;f+f_0) \tag{10}$$

and assuming that $2f_0 > W$, one obtains a simple approximation

$$\mathcal{E}\{Y_k(f_0)\} = \mu U_k(N,W;0) + \mu^* U_k(N,W;2f_0) \approx \mu U_k(N,W;0) \tag{11}$$

since $U_k(N,W;f)$ are maximally concentrated around $f = 0$ (Slepian; 1978). Complex magnitude μ could be estimated by minimizing error between the eigen spectrum $Y_k(f)$ and $\mu(f)U_k(N,W;0)$. The result of such minimization is a simple linear regression (Papoulis; 1991) of $Y_k(f)$ on $U_k(N,W;0)$ and is given by

$$\hat{\mu}(f) = \frac{1}{\sum_{k=0}^{K-1}|U_k(0)|^2}\sum_{k=0}^{K-1} U_k^*(0)Y_k(f) \tag{12}$$

The fact that the estimate $\hat{\mu}(f)$ is the linear regression allows to use standard regression F-test (Conover; 1998) for significance of the line component with amplitude $\hat{\mu}(f)$ at frequency f. This could be achieved by comparing the ration (Thomson; 1982)

$$F(f) = (K-1)\frac{|\hat{\mu}(f)|^2}{\epsilon^2(\hat{\mu},f)}\sum_{k=0}^{K-1}|U_k^*(0)|^2 \tag{13}$$

The location of the maximum (or local maxima) of $F(f)$ provides an estimate of the line component of the spectrum. The hypothesis that there is a line component with magnitude $\hat{\mu}(f_0)$ at $f = f_0$ is accepted if $F(f)$ has maximum at $f = f_0$ and

$$F(f_0) > F_\alpha(K) \tag{14}$$

where $F_\alpha(K)$ is the threshold for significance level α and $K-1$ degrees of freedom. Values of $F_\alpha(K)$ can be found in standard books on statistics (Conover; 1998).
Estimation of spectrum in the vicinity of a line spectrum component at $f = f_0$ is done according to the following equation

$$\hat{S}(f) = \frac{1}{K}\sum_{k=0}^{K-1} |Y_k(f) - \hat{\mu} V_k(f - f_0)|^2 \tag{15}$$

and

$$\hat{S}(f) = \frac{1}{K}\sum_{k=0}^{K-1} |Y_k(f)|^2 \tag{16}$$

otherwise.
It is recommended that the original sequence $x(n)$ is zero-padded to create a mesh of length $4-10$ times longer than the original N. This is essential to avoid missing a line spectrum component which is far from the grid frequency (Rao and Hamed; 2003).

2.2 Physical Model of Mobile-to-Mobile Channel

The propagation of electromagnetic waves in urban environments is a very complicated phenomenon (Beckmann and Spizzichino; 1963; Bertoni; 2000). The received waves are usually a combination of Line of Site (LoS) and a number of specular and diffusive components. Mobile-to-mobile communications (Sen and Matolak; 2008) introduce a new geometry of radio wave propagation, especially in urban settings. In such settings, antennas are located on a level well below rooftops or even tree-tops. Therefore propagation is dominated by rays reflected and diffracted from buildings, trees, other cars, etc. as in Fig. 1. Grazing angles are also often very small in such scenarios, therefore reflective surfaces cannot always be treated as smooth, resulting into LoS-like specular component, nor as very rough, resulting in a purely diffusive component (Beckmann and Spizzichino; 1963). It is also common to assume that, the resulting superposition of multiple reflected and diffused rays results into a spherically symmetric random process (Schreier and Scharf; 2003). However, it is shown in (Beckmann and Spizzichino; 1963), that there is an intermediate case which results in a partially coherent reflection, and, as such to improper complex Gaussian process, representing channel transfer function. When a number of reflected waves is not sufficient, the resulting distribution is highly non-Gaussian (Barakat; 1986). We defer investigation of such cases to future work and existing literature (Barakat; 1986), (Jakeman and Tough; 1987). Here we focus on the origin of the four-parametric distribution (Klovski; 1982) and estimation of its parameters.

2.2.1 Scattering from rough surfaces

Let us consider a rough surface of extent $2L \gg \lambda$ of the first Fresnel zone which is illuminated by a plane wave at the incidence angle $\theta_i = \pi/2 - \gamma$ as shown in Figs. 1-2.
We assume a simple Gaussian model of the surface roughness (Beckmann and Spizzichino; 1963), which is described by a random deviation $\zeta(x)$ from the mean level. The process $\zeta(x)$ has variance σ_r^2, the spatial covariance function $C(\Delta x) = \sigma_r^2 c(\Delta x)$, and the correlation length X (Beckmann and Spizzichino; 1963).
Let us consider first reflection from a surface portion of length X, equal to the correlation length of the roughness as shown in Fig. 2. Specular direction phases of elementary waves in specular direction have a random component

$$\eta_\phi = \frac{4\pi}{\lambda}\zeta(x)\cos\theta_i \tag{17}$$

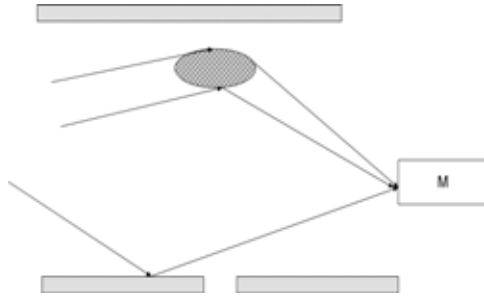

Fig. 1. Mobile-to-mobile propagation scenario. In addition to LoS and diffusive components (not shown) there are specular reflections from rough surfaces such as building facades and trees.

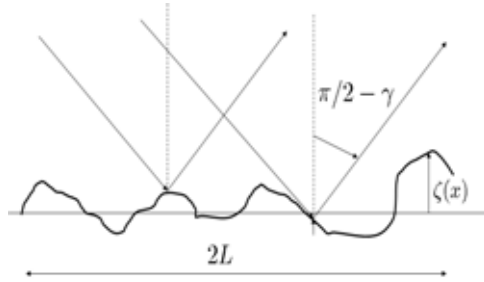

Fig. 2. Rough surface geometry. Size of the patch $2L$ corresponds to the size of the first Fresnel zone. Rough surface is described by a random process $\zeta(x)$.

Thus, the variance σ_ϕ^2 of the random phase deviation could be evaluated as

$$\sigma_\phi^2 = 16\pi^2 \frac{\sigma_r^2}{\lambda^2} \cos^2\theta_i \tag{18}$$

If $\sigma_\phi^2 \gg 4\pi^2$, *i.e.*

$$g = 2\frac{\sigma_r}{\lambda}\cos\theta_i \gg 1 \tag{19}$$

then the variation of phase is significantly larger then 2π. The distribution of the wrapped phase (Mardia and Jupp; 2000) is approximately uniform and the resulting wave could be considered as a purely diffusive component. However, in the opposite case of $0 < g \ll 1$ the variation of phase is significantly less then 2π and cannot be considered uniform. For a perfectly smooth surface $g = 0$ and the phase is deterministic, similar to LoS.
If the first Fresnel zone has extent $2L$, then there is approximately $N = 2L/X$ independent sections of the rough surface patches which contribute independently to the resultant field. Therefore, one can assume the following model for the reflected field/signal in the specular direction

$$\xi = \sum_{n=1}^{N} A_n \exp(j\phi_n) \tag{20}$$

where ϕ_n is a randomly distributed phase with the variance given by equation (18). If $\sigma_\phi^2 \gg 4\pi^2$ the model reduces to well accepted spherically symmetric diffusion component model; if $\sigma_\phi^2 = 0$, LoS-like conditions for specular component are observed with the rest of the values spanning an intermediate scenario.
Detailed investigation of statistical properties of the model, given by equation (20), can be found in (Beckmann and Spizzichino; 1963) and some consequent publications, especially in the field of optics (Barakat; 1986), (Jakeman and Tough; 1987). Assuming that the Central Limit Theorem holds, as in (Beckmann and Spizzichino; 1963), one comes to conclusion that $\xi = \xi_I + j\xi_Q$ is a Gaussian process with zero mean and *unequal* variances σ_I^2 and σ_Q^2 of the real and imaginary parts. Therefore ξ is an improper random process (Schreier and Scharf; 2003). Coupled with a constant term $m = m_I + jm_Q$ from the LoS type components, the model (20) gives rise to a large number of different distributions of the channel magnitude, including Rayleigh ($m = 0$, $\sigma_I = \sigma_Q$), Rice ($m \neq 0$, $\sigma_I = \sigma_Q$), Hoyt ($m \neq 0$, $\sigma_I > 0$ $\sigma_Q = 0$) and many others (Klovski; 1982), (Simon and Alouini; 2000). Following (Klovski; 1982) we will refer to the general case as a four-parametric distribution, defined by the following parameters

$$m = \sqrt{m_I^2 + m_Q^2},\ \phi = \arctan\frac{m_Q}{m_I} \tag{21}$$

$$q^2 = \frac{m_I^2 + m_Q^2}{\sigma_I^2 + \sigma_Q^2},\ \beta = \frac{\sigma_Q^2}{\sigma_I^2} \tag{22}$$

Two parameters, q^2 and β, are the most fundamental since they describe power ration between the deterministic and stochastic components (q^2) and asymmetry of the components (β). The further study is focused on these two parameters.

2.2.2 Channel matrix model

Let us consider a MIMO channel which is formed by N_T transmit and N_R received antennas. The $N_R \times N_T$ channel matrix

$$\mathbf{H} = \mathbf{H}_{LoS} + \mathbf{H}_{diff} + \mathbf{H}_{sp} \tag{23}$$

can be decomposed into three components. Line of sight component $\mathbf{H}_{LoS}$ could be represented as

$$\mathbf{H}_{LoS} = \sqrt{\frac{P_{LoS}}{N_T N_R}}\mathbf{a}_L \mathbf{b}_L^H \exp(j\phi_{LoS}) \tag{24}$$

Here P_{LoS} is power carried by LoS component, $\mathbf{a}_L$ and $\mathbf{b}_L$ are receive and transmit antenna manifolds (van Trees; 2002) and ϕ_{LoS} is a deterministic constant phase. Elements of both manifold vectors have unity amplitudes and describe phase shifts in each antenna with respect to some reference point[1]. Elements of the matrix $\mathbf{H}_{diff}$ are assumed to be drawn from proper (spherically-symmetric) complex Gaussian random variables with zero mean and correlation between its elements, imposed by the joint distribution of angles of arrival and departure (Almers et al.; 2006). This is due to the assumption that the diffusion component is composed of a large number of waves with independent and uniformly distributed phases due to large and rough scattering surfaces. Both LoS and diffusive components are well studied in the literature. Combination of the two lead to well known Rice model of MIMO channels (Almers et al.; 2006).

[1]This is not true when the elements of the antenna arrays are not identical or different polarizations are used.

Proper statistical interpretation of specular component $\mathbf{H}_{sp}$ is much less developed in MIMO literature, despite its applications in optics and random surface scattering (Beckmann and Spizzichino; 1963). The specular components represent an intermediate case between LoS and a purely diffusive component. Formation of such a component is often caused by mild roughness, therefore the phases of different partial waves have either strongly correlated phases or non-uniform phases.
In order to model contribution of specular components to the MIMO channel transfer function we consider first a contribution from a single specular component. Such a contribution could be easily written in the following form

$$\mathbf{H}_{sp} = \sqrt{\frac{P_{sp}}{N_T N_R}} \left[\mathbf{a} \odot \mathbf{w}_a\right] \left[\mathbf{b} \odot \mathbf{w}_b\right]^H \xi \tag{25}$$

Here P_{sp} is power of the specular component, $\xi = \xi_R + j\xi_I$ is a random variable drawn according to equation (20) from a complex Gaussian distribution with parameters $m_I + jm_Q$, σ_I^2, σ_Q^2 and independent in-phase and quadrature components. Since specular reflection from a moderately rough or very rough surface allows reflected waves to be radiated from the first Fresnel zone it appears as a signal with some angular spread. This is reflected by the window terms $\mathbf{w}_a$ and $\mathbf{w}_b$ (van Trees; 2002; Primak and Sejdić; 2008). It is shown in (Primak and Sejdić; 2008) that it could be well approximated by so called discrete prolate spheroidal sequences (DPSS) (Percival and Walden; 1993b) or by a Kaiser window (van Trees; 2002; Percival and Walden; 1993b). If there are multiple specular components, formed by different reflective rough surfaces, such as in an urban canyon in Fig. 1, the resulting specular component is a weighted sum of (25) like terms defined for different angles of arrival and departures:

$$\mathbf{H}_{sp} = \sum_{k=1} \sqrt{\frac{P_{sp,k}}{N_T N_R}} \left[\mathbf{a}_k \odot \mathbf{w}_{a,k}\right] \left[\mathbf{b}_k \odot \mathbf{w}_{b,k}\right]^H \xi_k \tag{26}$$

It is important to mention that in the mixture (26), unlike the LoS component, the absolute value of the mean term is not the same for different elements of the matrix $\mathbf{H}_{sp}$. Therefore, it is not possible to model them as identically distributed random variables. Their parameters (mean values) also have to be estimated individually. However, if the angular spread of each specular component is very narrow, the windows $\mathbf{w}_{a,k}$ and $\mathbf{w}_{b,k}$ could be assumed to have only unity elements. In this case, variances of the in-phase and quadrature components of all elements of matrix $\mathbf{H}_{sp}$ are the same.

3. MDPSS wideband simulator of Mobile-to-Mobile Channel

There are different ways of describing statistical properties of wide-band time-variant MIMO channels and their simulation. The most generic and abstract way is to utilize the time varying impulse response $\mathbf{H}(\tau, t)$ or the time-varying transfer function $\mathbf{H}(\omega, t)$ (Jeruchim et al.; 2000), (Almers et al.; 2006). Such description does not require detailed knowledge of the actual channel geometry and is often available from measurements. It also could be directly used in simulations (Jeruchim et al.; 2000). However, it does not provide good insight into the effects of the channel geometry on characteristics such as channel capacity, predictability, *etc.*. In addition such representations combine propagation environment with antenna characteristics into a single object.

An alternative approach, based on describing the propagation environment as a collection of scattering clusters is advocated in a number of recent publications and standards (Almers et al.; 2006; Asplund et al.; 2006). Such an approach gives rise to a family of so called Sum-Of-Sinusoids (SoS) simulators.
Sum of Sinusoids (SoS) or Sum of Cisoids (SoC) simulators (Patzold; 2002; SCM Editors; 2006) is a popular way of building channel simulators both in SISO and MIMO cases. However, this approach is not a very good option when prediction is considered since it represents a signal as a sum of coherent components with large prediction horizon (Papoulis; 1991). In addition it is recommended that up to 10 sinusoids are used per cluster. In this communication we develop a novel approach which allows one to avoid this difficulty. The idea of a simulator combines representation of the scattering environment advocated in (SCM Editors; 2006; Almers et al.; 2006; Molisch et al.; 2006; Asplund et al.; 2006; Molish; 2004) and the approach for a single cluster environment used in (Fechtel; 1993; Alcocer et al.; 2005) with some important modifications (Yip and Ng; 1997; Xiao et al.; 2005).

3.1 Single Cluster Simulator

3.1.1 Geometry of the problem

Let us first consider a single cluster scattering environment, shown in Fig. 2. It is assumed that both sides of the link are equipped with multielement linear array antennas and both are mobile. The transmit array has N_T isotropic elements separated by distance d_T while the receive side has N_R antennas separated by distance d_R. Both antennas are assumed to be in the horizontal plane; however extension on the general case is straightforward. The antennas are moving with velocities v_T and v_R respectively such that the angle between corresponding broadside vectors and the velocity vectors are α_T and α_R. Furthermore, it is assumed that the impulse response $H(\tau,t)$ is sampled at the rate F_{st}, *i.e.* $\tau = n/F_{st}$ and the channel is sounded with the rate F_s impulse responses per second, *i.e.* $t = m/F_s$. The carrier frequency is f_0. Practical values will be given in Section 4.
The space between the antennas consist of a single scattering cluster whose center is seen at the the azimuth ϕ_{0T} and co-elevation θ_T from the receiver side and the azimuth ϕ_{0R} and co-elevation θ_R. The angular spread in the azimuthal plane is $\Delta\phi_T$ on the receiver side and $\Delta\phi_R$ on the transmit side. No spread is assumed in the co-elevation dimension to simplify calculations due to a low array sensitivity to the co-elevation spread. We also assume that $\theta_R = \theta_T = \pi/2$ to shorten equations. Corresponding corrections are rather trivial and are omitted here to save space. The angular spread on both sides is assumed to be small comparing to the angular resolution of the arrays due to a large distance between the antennas and the scatterer (van Trees; 2002):

$$\Delta\phi_T \ll \frac{2\pi\lambda}{(N_T-1)d_T},\ \Delta\phi_R \ll \frac{2\pi\lambda}{(N_R-1)d_R}. \tag{27}$$

The cluster also assumed to produce certain delay spread variation, $\Delta\tau$, of the impulse response due to its finite dimension. This spread is assumed to be relatively small, not exceeding a few sampling intervals $T_s = 1/F_{st}$.

3.1.2 Statistical description

It is well known that the angular spread (dispersion) in the impulse response leads to spatial selectivity (Fleury; 2000) which could be described by corresponding covariance function

$$\rho(d) = \int_{-\pi}^{\pi} \exp\left(j2\pi\frac{d}{\lambda}\phi\right) p(\phi)d\phi \tag{28}$$

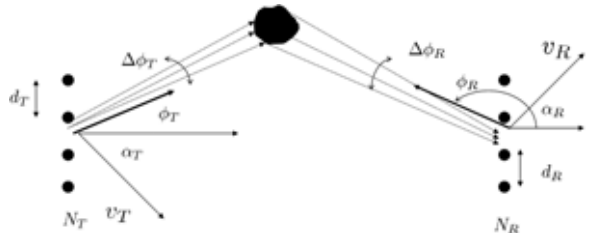

Fig. 3. Geometry of a single cluster problem.

where $p(\phi)$ is the distribution of the AoA or AoD. Since the angular size of clusters is assumed to be much smaller that the antenna angular resolution, one can further assume the following simplifications: a) the distribution of AoA/AoD is uniform and b) the joint distribution $p_2(\phi_T,\phi_R)$ of AoA/AoD is given by

$$p_2(\phi_T,\phi_R) = p_{\phi_T}(\phi_T)p_{\phi_R}(\phi_R) = \frac{1}{\Delta_{\phi_T}} \cdot \frac{1}{\Delta_{\phi_R}} \tag{29}$$

It was shown in (Salz and Winters; 1994) that corresponding spatial covariance functions are modulated sinc functions

$$\rho(d) \approx \exp\left(j\frac{2\pi d}{\lambda}\sin\phi_0\right)\operatorname{sinc}\left(\Delta\phi\frac{d}{\lambda}\cos\phi_0\right) \tag{30}$$

The correlation function of the form (30) gives rise to a correlation matrix between antenna elements which can be decomposed in terms of frequency modulated Discrete Prolate Spheroidal Sequences (MDPSS) (Alcocer et al.; 2005; Slepian; 1978; Sejdić et al.; 2008):

$$\mathbf{R} \approx \mathbf{W}\mathbf{U}\Lambda\mathbf{U}^H\mathbf{W}^H = \sum_{k=0}^{D}\lambda_k\mathbf{u}_k\mathbf{u}_k^H \tag{31}$$

where $\Lambda \approx \mathbf{I}_D$ is the diagonal matrix of size $D \times D$ (Slepian; 1978), $\mathbf{U}$ is $N \times D$ matrix of the discrete prolate spheroidal sequences and $\mathbf{W} = \operatorname{diag}\{\exp(j2\pi d/\lambda \sin nd_A)\}$. Here d_A is distance between the antenna elements, N number of antennas, $1 \le n \le N$ and $D \approx \lceil 2\Delta\phi\frac{d}{\lambda}\cos\phi_0\rceil + 1$ is the effective number of degrees of freedom generated by the process with the given covariance matrix $\mathbf{R}$. For narrow spread clusters the number of degrees of freedom is much less than the number of antennas $D \ll N$ (Slepian; 1978). Thus, it could be inferred from equation (31) that the desired channel impulse response $\mathbf{H}(\omega,\tau)$ could be represented as a double sum(tensor product).

$$\mathbf{H}(\omega,t) = \sum_{n_t}^{D_T}\sum_{n_r}^{D_R}\sqrt{\lambda_{n_t}\lambda_{n_r}}\mathbf{u}_{n_r}^{(r)}\mathbf{u}_{n_t}^{(t)^H}h_{n_t,n_r}(\omega,t) \tag{32}$$

In the extreme case of a very narrow angular spread on both sides, $D_R = D_T = 1$ and $\mathbf{u}_1^{(r)}$ and $\mathbf{u}_1^{(t)}$ are well approximated by the Kaiser windows (Thomson; 1982). The channel corresponding to a single scatterer is of course a rank one channel given by

$$\mathbf{H}(\omega,t) = \mathbf{u}_1^{(r)}\mathbf{u}_1^{(t)^H}h(\omega,t). \tag{33}$$

Considering the shape of the functions $\mathbf{u}_1^{(r)}$ and $\mathbf{u}_1^{(t)}$ one can conclude that in this scenario angular spread is achieved by modulating the amplitude of the spatial response of the channel on both sides. It is also worth noting that representation (32) is the Karhunen-Loeve series (van Trees; 2001) in spatial domain and therefore produces smallest number of terms needed to represent the process selectivity in spatial domain. It is also easy to see that such modulation becomes important only when the number of antennas is significant.
Similar results could be obtained in frequency and Doppler domains. Let us assume that τ is the mean delay associated with the cluster and $\Delta\tau$ is corresponding delay spread. In addition let it be desired to provide a proper representation of the process in the bandwidth $[-W:W]$ using N_F equally spaced samples. Assuming that the variation of power is relatively minor within $\Delta\tau$ delay window, we once again recognize that the variation of the channel in frequency domain can be described as a sum of modulated DPSS of length N_F and the time bandwidth product $W\Delta\tau$. The number of MDPSS needed for such representation is approximately $D_F = 2W\Delta\tau + 1$ (Slepian; 1978):

$$\mathbf{h}(\omega,t) = \sum_{n_f=1}^{D_f} \sqrt{\lambda_{nf}}\mathbf{u}_{n_f}^{(\omega)} h_{n_f}(t) \tag{34}$$

Finally, in the Doppler domain, the mean resulting Doppler spread could be calculated as

$$f_D = \frac{f_0}{c}\left[v_T\cos\left(\phi_{T0}-\alpha_T\right) + v_R\cos\left(\phi_{R0}-\alpha_R\right)\right]. \tag{35}$$

The angular extent of the cluster from sides causes the Doppler spectrum to widen by the folowing

$$\Delta f_D = \frac{f_0}{c}\left[v_T\Delta\phi_T v_T|\sin\left(\phi_{T0}-\alpha_T\right)| + v_R\Delta\phi_R|\sin\left(\phi_{R0}-\alpha_R\right)|\right]. \tag{36}$$

Once again, due to a small angular extent of the cluster it could be assumed that the widening of the Doppler spectrum is relatively narrow and no variation within the Doppler spectrum is of importance. Therefore, if it is desired to simulate the channel on the interval of time $[0:T_{max}]$ then this could be accomplished by adding $D = 2\Delta f_D Tmax + 1$ MDPS:

$$\mathbf{h}_d = \sum_{n_d=0}^{D} \xi_{n_d}\sqrt{\lambda_{n_d}}\mathbf{u}_{n_d}^{(d)} \tag{37}$$

where ξ_{n_d} are independent zero mean complex Gaussian random variables of unit variance.
Finally, the derived representation could be summarized in tensor notation as follows. Let $\mathbf{u}_{n_t}^{(t)}$, $\mathbf{u}_{n_r}^{(r)}$, $\mathbf{u}_{n_f}^{(\omega)}$ and $\mathbf{u}_{n_d}^{(d)}$ be DPSS corresponding to the transmit, receive, frequency and Doppler dimensions of the signal with the "domain-dual domain" products (Slepian; 1978) given by $\Delta\phi_T\frac{d}{\lambda}\cos\phi_{T0}$, $\Delta\phi_R\frac{d}{\lambda}\cos\phi_{R0}$, $W\Delta\tau$ and $T_{max}\Delta f_D$ respectively. Then a sample of a MIMO frequency selective channel with corresponding characteristics could be generated as

$$\mathcal{H}_4 = \mathcal{W}_4 \odot \sum_{n_t}^{D_T}\sum_{n_r}^{D_R}\sum_{n_f}^{D_F}\sum_{n_d}^{d}\sqrt{\lambda_{n_t}^{(t)}\lambda_{n_r}^{(r)}\lambda_{n_f}^{(\omega)}\lambda_{n_d}^{(T)}}\xi_{n_t,n_r,n_f,n_d}\cdot$$
$$\cdot\, {}_1\mathbf{u}_{n_t}^{(r)} \times {}_2\mathbf{u}_{n_r}^{(r)} \times {}_3\mathbf{u}_{n_f}^{(\omega)} \times {}_4\mathbf{u}_{n_d}^{(d)} \tag{38}$$

where $\mathcal{W}_4$ is a tensor composed of modulating sinusoids

$$\mathcal{W}_4 = {}_1\mathbf{w}^{(r)} \times {}_2\mathbf{w}^{(t)} \times {}_3\mathbf{w}^{(\omega)} \times {}_4\mathbf{w}^{(d)} \tag{39}$$

$$\begin{aligned}
\mathbf{w}^{(r)} &= \left[1, \exp\left(j2\pi\frac{d_R}{\lambda}\right), \cdots, \exp\left(j2\pi\frac{d_R}{\lambda}(N_R-1)\right)\right]^T \\
\mathbf{w}^{(t)} &= \left[1, \exp\left(j2\pi\frac{d_T}{\lambda}\right), \cdots, \exp\left(j2\pi\frac{d_T}{\lambda}(N_T-1)\right)\right]^T
\end{aligned} \tag{40}$$

$$\begin{aligned}
\mathbf{w}^{(\omega)} &= \left[1, \exp\left(j2\pi\Delta F\tau\right), \cdots, \exp\left(j2\pi\Delta F(N_F-1)\right)\right]^T \\
\mathbf{w}^{(d)} &= \left[1, \exp\left(j2\pi\Delta f_D T_s\right), \cdots, \exp\left(j2\pi\Delta f_D(T_{max}-T_s)\right)\right]^T
\end{aligned} \tag{41}$$

and $\odot$ is the Hadamard (element wise) product of two tensors (van Trees; 2002).

3.2 Multi-Cluster environment

The generalization of the model suggested in Section 3.1 to a real multi-cluster environment is straightforward. The channel between the transmitter and the receiver is represented as a set of clusters, each described as in Section (3.1). The total impulse response is superposition of independently generated impulse response tensors from each cluster

$$\mathcal{H}_4 = \sum_{k=0}^{N_c-1} \sqrt{P_k}\mathcal{H}_4(k), \sum_{k=1}^{N_c} P_k = P \tag{42}$$

where N_c is the total number of clusters, $\mathcal{H}_4(k)$ is a normalized response from the k-th cluster $||\mathcal{H}_4(k)||_F^2 = 1$ and $P_k \geq 0$ represents relative power of k-th cluster and P is the total power.
It is important to mention here that such a representation does not necessarily correspond to a physical cluster distribution. It rather reflects interplay between radiated and received signals, arriving from certain direction with a certain excess delay, ignoring particular mechanism of propagation. Therefore it is possible, for example, to have two clusters with the same AoA and AoD but a different excess delay. Alternatively, it is possible to have two clusters which correspond to the same AoD and excess delay but very different AoA.
Equations (38) and (42) reveal a connection between Sum of Cisoids (SoC) approach (SCM Editors; 2006) and the suggested algorithms: one can consider (38) as a modulated Cisoid. Therefore, the simulator suggested above could be considered as a Sum of Modulated Cisoids simulator.
In addition to space dispersive components, the channel impulse response may contain a number of highly coherent components, which can be modelled as pure complex exponents. Such components described either direct LoS path or specularly reflected rays with very small phase diffusion in time. Therefore equation (42) should be modified to account for such components:

$$\mathcal{H}_4 = \sqrt{\frac{1}{1+K}} \sum_{k=0}^{N_c-1} \sqrt{P_{ck}}\mathcal{H}_4(k) + \sqrt{\frac{K}{1+K}} \sum_{k=0}^{N_s-1} \sqrt{P_{sk}}\mathcal{W}_4(k) \tag{43}$$

Here N_s is a number of specular components including LoS and K is a generalized Rice factor describing ratio between powers of specular P_{sk} and non-coherent/diffusive components P_{ck}

$$K = \frac{\sum_{k=0}^{N_s-1} P_{sk}}{\sum_{k=0}^{N_c-1} P_{ck}} \tag{44}$$

While distribution of the diffusive component is Gaussian by construction, the distribution of the specular component may not be Gaussian. A more detailed analysis is beyond the scope of this chapter and will be considered elsewhere. We also leave a question of identifying and distinguishing coherent and non-coherent components to a separate manuscript.

4. Examples

Fading channel simulators (Jeruchim et al.; 2000) can be used for different purposes. The goal of the simulation often defines not only suitability of a certain method but also dictates choice of the parameters. One possible goal of simulation is to isolate a particular parameter and study its effect of the system performance. Alternatively, a various techniques are needed to avoid the problem of using the same model for both simulation and analysis of the same scenario. In this section we provide a few examples which show how suggested algorithm can be used for different situations.

4.1 Two cluster model

The first example we consider here is a two-cluster model shown in Fig. 4. This geometry is

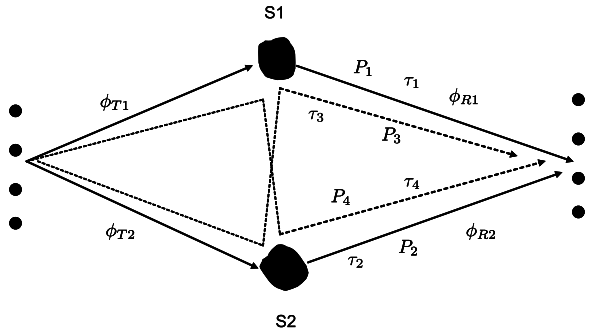

Fig. 4. Geometry of a single cluster problem.

the simplest non-trivial model for frequency selective fading. However, it allows one to study effects of parameters such as angular spread, delay spread, correlation between sites on the channel parameters and a system performance. The results of the simulation are shown in Figs. 5-6. In this examples we choose $\phi_{T1} = 20^o$, $\phi_{T2} = 20^o$, $\phi_{R1} = 0^o$, $\phi_{R2} = 110^o$, $\tau_1 = 0.2\,\mu s$, $\tau_2 = 0.4\,\mu s$, $\Delta\tau_1 = 0.2\,\mu s$, $\Delta\tau_2 = 0.4\,\mu s$.

4.2 Environment specified by joint AoA/AoD/ToA distribution

The most general geometrical model of MIMO channel utilizes joint distribution $p(\phi_T, \phi_R, \tau)$, $0 \leq \phi_T < 2\pi$, $0 \leq \phi_R < 2\pi$, $\tau_{min} \leq \tau \leq \tau_{max}$, of AoA, AoD and Time of Arrival (ToA). A few of such models could be found in the literature (Kaiserd et al.; 2006), (Andersen and Blaustaein; 2003; Molisch et al.; 2006; Asplund et al.; 2006; Blaunstein et al.; 2006; Algans et al.; 2002). Theoretically, this distribution completely describes statistical properties of the MIMO channel. Since the resolution of the antenna arrays on both sides is finite and a finite bandwidth of the channel is utilized, the continuous distribution $p(\phi_T, \phi_R, \tau)$ can be discredited to produce narrow "virtual" clusters centered at $[\phi_{Tk}, \phi_{Rk}, \tau_k]$ and with spread $\Delta\phi_{Tk}$, $\Delta\phi_{Rk}$ and $\Delta\tau_k$

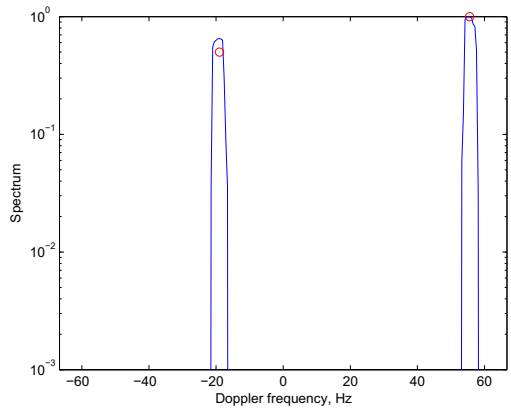

Fig. 5. PSD of the two cluster channel response.

respectively and the power weight

$$P_k = \frac{P}{4\pi^2(\tau_{max} - \tau_{min})} \times \int_{\tau_k - \Delta\tau_k/2}^{\tau_k + \Delta\tau_k/2} d\tau \int_{\phi_{Tk} - \Delta\phi_{Tk}/2}^{\phi_{Tk} + \Delta\phi_{Tk}/2} d\phi_T \int_{\phi_{Rk} - \Delta\phi_{Rk}/2}^{\phi_{Rk} + \Delta\phi_{Rk}/2} p(\phi_T, \phi_R, \tau) d\phi_R \quad (45)$$

We omit discussions about an optimal partitioning of each domain due to the lack of space. Assume that each virtual cluster obtained by such partitioning is appropriate in the frame discussed in Section 3.1.

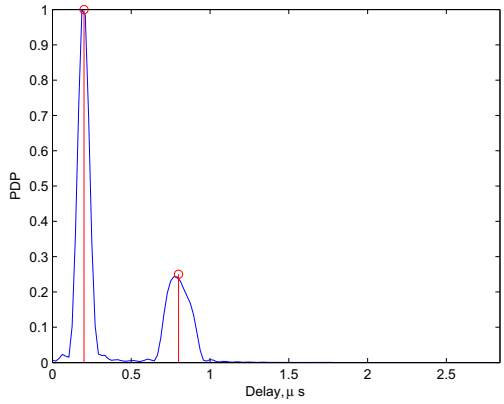

Fig. 6. PDP of the two cluster channel response.

As an example, let us consider the following scenario, described in (Blaunstein et al.; 2006). In this case the effect of the two street canyon propagation results into two distinct angles

of arrival $\phi_{R1} = 20^o$ and $\phi_{R2} = 50^o$, AoA spreads roughly of $\Delta_1 = \Delta_2 = 5^o$ and exponential PDP corresponding to each AoA (see Figs. 5 and 6 in (Blaunstein et al.; 2006)). In addition, an almost uniform AoA on the interval $[60 : 80^o]$ corresponds to early delays. Therefore, a simplified model of such environment could be presented by

$$p(\phi_R,\tau) = \sqrt{P_1}\frac{1}{\Delta_1}\exp\left(-\frac{\tau-\tau_1}{\tau_{s1}}\right)u(\tau-\tau_1)+ \\ \sqrt{P_2}\frac{1}{\Delta_2}\exp\left(-\frac{\tau-\tau_2}{\tau_{s2}}\right)u(\tau-\tau_2)+\sqrt{P_3}\frac{1}{\Delta_3}\exp\left(-\frac{\tau-\tau_3}{\tau_{s3}}\right)u(\tau-\tau_3) \quad (46)$$

where $u(t)$ is the unit step function, τ_{sk}, $k = 1,2,3$ describe rate of decay of PDP. By inspection of Figs. 5-6 in (Blaunstein et al.; 2006) we choose $\tau_1 = \tau_2 = 1.2$ ns, $\tau_3 = 1.1$ ns and $\tau_{s1} = \tau_{s2} = \tau_{s3} = 0.3$ ns. Similarly, by inspection of the same figures we assume $P_1 = P_2 = 0.4$ and $P_3 = 0.2$. To model exponential PDP with unit power and average duration τ_s we represent it with a set of $N \geq 1$ rectangular PDP of equal energy $1/N$. The k-th virtual cluster then extends on the interval $[\tau_{k-1} : \tau_k]$ and has magnitude $P_k = 1/N\Delta\tau_k$ where $\tau_0 = 0$

$$\tau_k = \tau_s \ln\frac{N-k}{N},\ k = 1,...,N-1 \quad (47)$$

$$\tau_N = \tau_{N-1} + \frac{1}{N\tau_{N-1}},\ k = N \quad (48)$$

$$\Delta\tau_k = \tau_k - \tau_{k-1} \quad (49)$$

Results of numerical simulation are shown in Figs. 7 and 8. It can be seen that a good agreement between the desired characteristics is obtained.

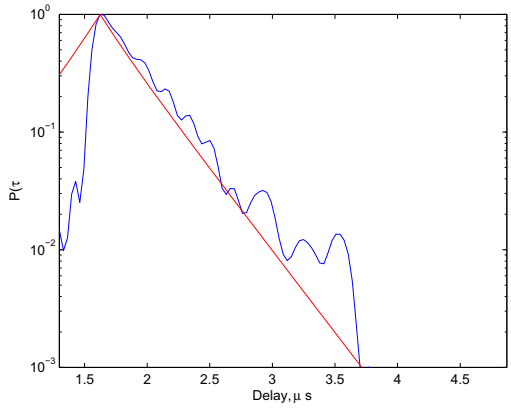

Fig. 7. Simulated power delay profile for the example of Section 4.2.

Similarly, the same technique could be applied to the 3GPP (SCM Editors; 2006) and COST 259 (Asplund et al.; 2006) specifications.

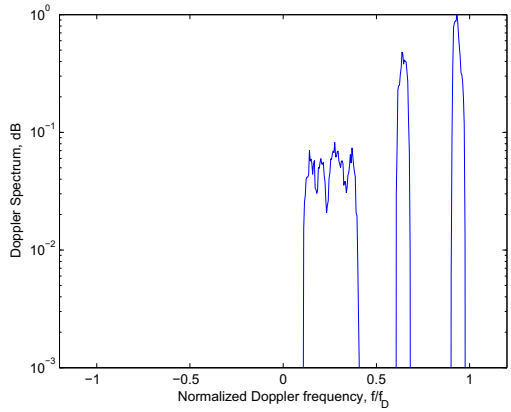

Fig. 8. Simulated Doppler power spectral density for the example of Section 4.2.

5. MDPSS Frames for channel estimation and prediction

5.1 Modulated Discrete Prolate Spheroidal Sequences

If the DPSS are used for channel estimation, then usually accurate and sparse representations are obtained when both the DPSS and the channel under investigation occupy the same frequency band (Zemen and Mecklenbräuker; 2005). However, problems arise when the channel is centered around some frequency $|\nu_o| > 0$ and the occupied bandwidth is smaller than $2W$, as shown in Fig. 9.

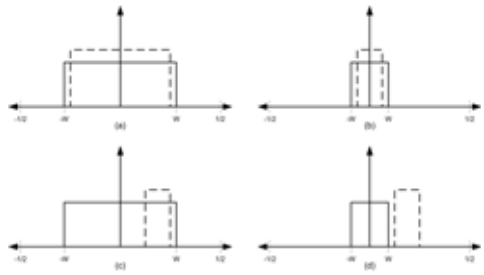

Fig. 9. Comparison of the bandwidth for a DPSS (solid line) and a channel (dashed line): (a) both have a wide bandwidth; (b) both have narrow bandwidth; (c) a DPSS has a wide bandwidth, while the channel's bandwidth is narrow and centered around $\nu_o > 0$; (d) both have narrow bandwidth, but centered at different frequencies.

In such situations, a larger number of DPSS is required to approximate the channel with the same accuracy despite the fact that such narrowband channel is more predictable than a wider band channel (Proakis; 2001). In order to find a better basis we consider so-called Modulated Discrete Prolate Spheroidal Sequences (MDPSS), defined as

$$M_k(N,W,\omega_m;n) = \exp(j\omega_m n)v_k(N,W;n), \tag{50}$$

where $\omega_m = 2\pi\nu_m$ is the modulating frequency. It is easy to see that MDPSS are also doubly orthogonal, obey the same equation (7) and are bandlimited to the frequency band $[-W+\nu : W+\nu]$.
The next question which needs to be answered is how to properly choose the modulation frequency ν. In the simplest case when the spectrum $S(\nu)$ of the channel is confined to a known band $[\nu_1;\nu_2]$, *i.e.*

$$S(\nu) = \begin{cases} \gg 0 & \forall \nu \in [\nu_1, \nu_2] \text{ and } |\nu_1| < |\nu_2| \\ \approx 0 & \text{elsewhere} \end{cases}, \tag{51}$$

the modulating frequency, ν_m, and the bandwidth of the DPSS's are naturally defined by

$$\nu_m = \frac{\nu_1 + \nu_2}{2} \tag{52}$$

$$W = \left| \frac{\nu_2 - \nu_1}{2} \right|, \tag{53}$$

as long as both satisfy:

$$|\nu_m| + W < \frac{1}{2}. \tag{54}$$

In practical applications the exact frequency band is known only with a certain degree of accuracy. In addition, especially in mobile applications, the channel is evolving in time. Therefore, only some relatively wide frequency band defined by the velocity of the mobile and the carrier frequency is expected to be known. In such situations, a one-band-fits-all approach may not produce a sparse and accurate approximation of the channel. To resolve this problem, it was previously suggested to use a band of bases with different widths to account for different speeds of the mobile (Zemen et al.; 2005). However, such a representation once again ignores the fact that the actual channel bandwidth $2W$ could be much less than $2\nu_D$ dictated by the maximum normalized Doppler frequency $\nu_D = f_D T$.
To improve the estimator robustness, we suggest the use of multiple bases, better known as frames (Kovačević and Chabira; 2007), precomputed in such a way as to reflect various scattering scenarios. In order to construct such multiple bases, we assume that a certain estimate (or rather its upper bound) of the maximum Doppler frequency ν_D is available. The first few bases in the frame are obtained using traditional DPSS with bandwidth $2\nu_D$. Additional bases can be constructed by partitioning the band $[-\nu_D;\nu_D]$ into K subbands with the boundaries of each subband given by $[\nu_k;\nu_{k+1}]$, where $0 \leq k \leq K-1$, $\nu_{k+1} > \nu_k$, and $\nu_0 = -\nu_D$, $\nu_{K-1} = \nu_D$. Hence, each set of MDPSS has a bandwidth equal to $\nu_{k+1} - \nu_k$ and a modulation frequency equal to $\nu_m = 0.5(\nu_k + \nu_{k+1})$. Obviously, a set of such functions again forms a basis of functions limited to the bandwidth $[-\nu_D;\nu_D]$. It is a convention in the signal processing community to call each basis function *an atom*. While particular partition is arbitrary for every level $K \geq 1$, we can choose to partition the bandwidth into equal blocks to reduce the amount of stored precomputed DPSS, or to partition according to the angular resolution of the receive antenna, *etc*, as shown in Fig. 10.
Representation in the overcomplete basis can be made sparse due to the richness of such a basis. Since the expansion into simple bases is not unique, a fast, convenient and unique projection algorithm cannot be used. Fortunately, efficient algorithms, known generically as pursuits (Mallat; 1999; Mallat and Zhang; 1993), can be used and they are briefly described in the next section.

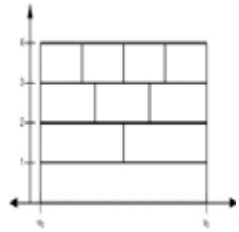

Fig. 10. Sample partition of the bandwidth for $K = 4$.

5.2 Matching Pursuit with MDPSS frames

From the few approaches which can be applied for expansion in overcomplete bases, we choose the so-called matching pursuit (Mallat and Zhang; 1993). The main feature of the algorithm is that when stopped after a few steps, it yields an approximation using only a few atoms (Mallat and Zhang; 1993). The matching pursuit was originally introduced in the signal processing community as an algorithm that decomposes any signal into a linear expansion of waveforms that are selected from a redundant dictionary of functions (Mallat and Zhang; 1993). It is a general, greedy, sparse function approximation scheme based on minimizing the squared error, which iteratively adds new functions (i.e. basis functions) to the linear expansion. In comparison to a basis pursuit, it significantly reduces the computational complexity, since the basis pursuit minimizes a global cost function over all bases present in the dictionary (Mallat and Zhang; 1993). If the dictionary is orthogonal, the method works perfectly. Also, to achieve compact representation of the signal, it is necessary that the atoms are representative of the signal behavior and that the appropriate atoms from the dictionary are chosen.
The algorithm for the matching pursuit starts with an initial approximation for the signal, $\widehat{x}$, and the residual, R:

$$\widehat{x}^{(0)} = 0 \tag{55}$$

$$R^{(0)} = x \tag{56}$$

and it builds up a sequence of sparse approximation stepwise by trying to reduce the norm of the residue, $R = \widehat{x} - x$. At stage k, it identifies the dictionary atom that best correlates with the residual and then adds to the current approximation a scalar multiple of that atom, such that

$$\widehat{x}^{(k)} = \widehat{x}^{(k-1)} + \alpha_k \phi_k \tag{57}$$

$$R^{(k)} = x - \widehat{x}^{(k)}, \tag{58}$$

where $\alpha_k = \langle R^{(k-1)}, \phi_k \rangle / \|\phi_k\|^2$. The process continues until the norm of the residual $R^{(k)}$ does not exceed required margin of error $\epsilon > 0$: $||R^{(k)}|| \leq \epsilon$ (Mallat and Zhang; 1993). In our approach, a stopping rule mandates that the number of bases, χ_B, needed for signal approximation should satisfy $\chi_B \leq \lceil 2N\nu_D \rceil + 1$. Hence, a matching pursuit approximates the signal using χ_B bases as

$$x = \sum_{n=1}^{\chi_B} \langle x, \phi_n \rangle \phi_n + R^{(\chi_B)}, \tag{59}$$

where ϕ_n are χ_B bases from the dictionary with the strongest contributions.

6. Numerical Simulation

In this section, the performance of the MDPSS estimator is compared with the Slepian basis expansion DPSS approach (Zemen and Mecklenbräuker; 2005) for a certain radio environment. The channel model used in the simulations is presented in Section 2.2 and it is simulated using the AR approach suggested in (Baddour and Beaulieu; 2005). The parameters of the simulated system are the same as in (Zemen and Mecklenbräuker; 2005): the carrier frequency is 2 GHz, the symbol rate used is 48600 $1/s$, the speed of the user is 102.5 km/h, 10 pilots per data block are used, and the data block length is $M = 256$. The number of DPSS's used in estimation is given by $\lceil 2M\nu_D \rceil + 1$. The same number of bases is used for MDPSS, while $K = 15$ subbands is used in generation of MDPSS.

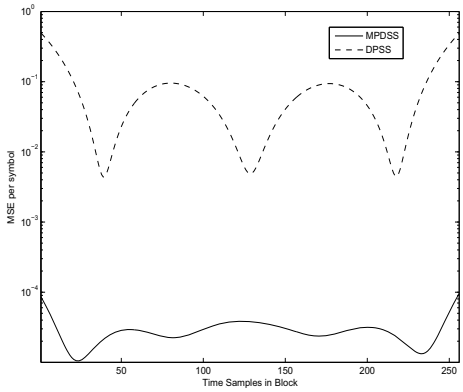

Fig. 11. Mean square error per symbol for MDPSS (solid) and DPSS (dashed) mobile channel estimators for the noise-free case.

As an introductory example, consider the estimation accuracy for the WSSUS channel with a uniform power angle profile (PAS) with central AoA $\phi_0 = 5$ degrees and spread $\Delta = 20$ degrees. We used 1000 channel realizations and Fig. 11 depicts the results for the considered channel model. The mean square errors (MSE) for both MDPSS and DPSS estimators have the highest values at the edges of the data block. However, the MSE for MDPSS estimator is several orders of magnitude lower than the value for the Slepian basis expansion estimator based on DPSS.

Next, let's examine the estimation accuracy for the WSSUS channels with uniform PAS, central AoAs $\phi_1 = 45$ and $\phi_1 = 75$, and spread $0 < \Delta \leq 2\pi/3$. Furthermore, it is assumed that the channel is noisy. Figs. 12 and 13 depict the results for $SNR = 10$ dB and $SNR = 20$ dB, respectively.

The results clearly indicate that the MDPSS frames are a more accurate estimation tool for the assumed channel model. For the considered angles of arrival and spreading angles, the MDPSS estimator consistently provided lower MSE in comparison to the Slepian basis expansion estimator based on DPSS. The advantage of the MDPSS stems from the fact that these bases are able to describe different scattering scenarios.

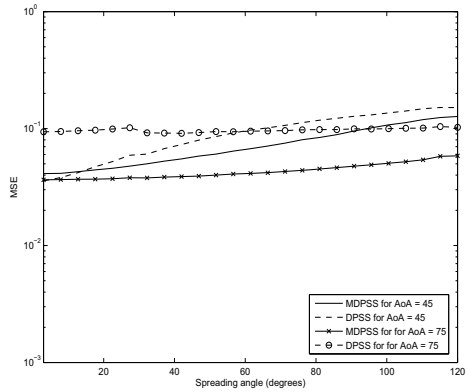

Fig. 12. Dependence of the MSE on the angular spread Δ and the mean angle of arrival for $SNR = 10$ dB.

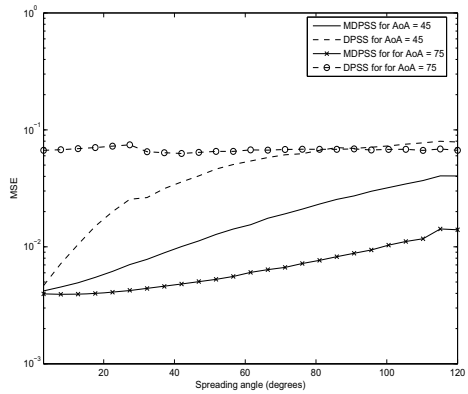

Fig. 13. Dependence of the MSE on the angular spread Δ and the mean angle of arrival for $SNR = 20$ dB.

7. Conclusions

In this Chapter we have presented a novel approach to modelling MIMO wireless communication channels. At first, we have argued that in most general settings the distribution of the in-phase and quadrature components are Gaussian but may have different variance. This was explained by an insufficient phase randomization by small scattering areas. This model leads to a non-Rayleigh/non-Rice distribution of magnitude and justifies usage of such generic distributions as Nakagami or Weibull. It was also shown that additional care should be taken when modelling specular components in MIMO settings.
Furthermore, based on the assumption that the channel is formed by a collection of relatively small but non-point scatterers, we have developed a model and a simulation tool to represent such channels in an orthogonal basis, composed of modulated prolate spheroidal sequences.
Finally MDPSS frames are proposed for estimation of fast fading channels in order to preserve sparsity of the representation and enhance the estimation accuracy. The members of the frame

were obtained by modulation and bandwidth variation of DPSS's in order to reflect various scattering scenarios. The matching pursuit approach was used to achieve a sparse representation of the channel. The proposed scheme was tested for various mobile channels, and its performance was compared with the Slepian basis expansion estimator based on DPSS. The results showed that the MDPSS method provides more accurate estimation than the DPSS scheme.

8. References

Alcocer, A., Parra, R. and Kontorovich, V. (2005). An orthogonalization approach for communication channel modelling, *Proc. VTC-2005, Fall*.

Alcocer-Ochoa, A., Kontorovitch, V. Y. and Parra-Michel, R. (2006). A MIMO channel simulator applying the universal basis, *Proc. of 64th IEEE Vehicular Technology Conference (VTC-2006)*, Montreal, QC, Canada.

Algans, A., Pedersen, K. and Mogensen, P. (2002). Experimental analysis of the joint statistical properties of azimuth spread, delay spread, and shadow fading, *IEEE J. Sel. Areas Commun.* **20**(3): 523–531.

Almers, P., Bonek, E., Burr, A., Czink, N., Debbah, M., Degli-Esposti, V., Hofstetter, H., Kyösti, P., Laurenson, D., Matz, G., Molisch, A. F., Oestges, C. and Özcelik, H. (2006). Survey of channel and radio propagation models for wireless mimo systems.

Andersen, J. and Blaustaein, N. (2003). *Multipath Phenomena in Cellular Networks*, Artech House, 2002.

Asplund, H., Glazunov, A., Molisch, A., Pedersen, K. and Steinbauer, M. (2006). The COST 259 directional channel model Part II: Macrocell, *IEEE Trans. Wireless Commun.* **5**(12): 3434–3450.

Baddour, K. E. and Beaulieu, N. C. (2005). Autoregressive modeling for fading channel simulation, *IEEE Transactions on Wireless Communications* **4**(4): 1650 – 1662.

Barakat, R. (1986). Weak-scatterer generalization of the *k*-density function with application to laser scattering in atmospheric turbulence, *J. Opt. Soc. Am. A* **3**(4): 401–409.

Beckmann, P. and Spizzichino, A. (1963). *The scattering of electromagnetic waves from rough surfaces*, Pergamon Press, New York, USA.

Bertoni, H. (2000). *Radio Propagation For Modern Wireless Systems*, Prentice Hall PTR, Upper Saddle River, NJ.

Blaunstein, N., Toeltsch, M., Laurila, J., Bonek, E., Katz, D., Vainikainen, P., Tsouri, N., Kalliola, K. and Laitinen, H. (2006). Signal power distribution in the azimuth, elevation and time delay domains in urban environments for various elevations of base station antenna, *IEEE Trans. Antennas Propag.* **54**(10): 2902.

Bronez, T. (1992). On the performance advantage of multitaper spectral analysis, *IEEE Trans. Signal Process.* **40**(12): 2941–2946.

Conover, W. (1998). *Practical Nonparametric Statistics*, third edn, Wiley, New York.

Fancourt, C. and Principe, J. (2000). On the relationship between the Karhunen-Loeve transform and the prolate spheroidal wave functions, *Proc. ICASSP 00*, Istambul, Turkey, pp. 261–264.

Fechtel, S. (1993). A novel approach to modeling and efficient simulation offrequency-selective fading radio channels, *IEEE J. Sel. Areas Commun.* **11**(3): 422–431.

Fleury, B. (2000). First- and second-order characterization of direction dispersion and space selectivity in the radio channel, *IEEE Trans. Inf. Theory* **46**(6): 2027–2044.

Jakeman, E. and Tough, R. (1987). Generalized *k* distribution: a statistical model for weak scattering, *J. Opt. Soc. Am. A* **4**(9): 1764–1772.

Jeruchim, M. C., Balaban, P. and Shanmugan, K. S. (2000). *Simulation of Communication Systems: Modeling, Methodology and Techniques*, New York: Springer.

Kaiserd, T., Bourdoux, A., Boche, H., Fonollosa, J., Andersen, J. and Utschick, W. (2006). *Smart Antennas: State of the Art*, Hindawi, NY.

Kirsteins, I., Mehta, S. and Fay, J. (2006). Adaptive separation of unknown narrowband and broadband time series, *Proc. ICASSP 98*, Seatlle, WA, USA, pp. 2525–2528.

Klovski, D. (1982). *Digital Data Transmission over Radiochannels*, Sviaz, Moscow, USSR, (in Russian).

Kontorovich, V., Primak, S., Alcocer-Ochoa1, A. and Parra-Michel, R. (2008). Mimo channel orthogonalisations applyinguniversal eigenbasis, *Proc. IET Signal processing* **2**(2): 87–96.

Kovačević, J. and Chabira, A. (2007). Life beyond bases: The advent of the frames (part I), *IEEE Signal Processing Magazine* **24**(4): 86–104.

Mallat, S. G. (1999). *A Wavelet Tour of Signal Processing*, second edn, Academic Press, San Diego.

Mallat, S. G. and Zhang, Z. (1993). Matching pursuits with time-frequency dictionaries, *IEEE Transactions on Signal Processing* **41**(12): 3397–3415.

Mardia, K. and Jupp, P. (2000). *Directional statistics*, Wiley, New York.

Molisch, A. F., Asplund, H., Heddergott, R., Steinbauer, M. and Zwick, T. (2006). The COST 259 directional channel model Part I: overview and methodology, *IEEE Trans. Wireless Commun.* **5**(12): 3421–3433.

Molish, A. (2004). A generic model for MIMO wireless propagation channels in macro- and microcells, *IEEE Trans. Signal Process.* **52**(1): 61–71.

Papoulis, A. (1991). *Probability, Random Variables, and Stochastic Processes*, third edn, McGraw-Hill, Boston, MA.

Patzold, M. (2002). *Mobile Fading Channels*, John Wiley & Sons, New York.

Percival, D. B. and Walden, A. T. (1993a). *Spectral Analysis for Physical Applications: Multitaper and Conventional Univeriate Techniques*, Cambridge University Press, New York.

Percival, D. and Walden, A. (1993b). *Spectral Analysis for Physical Applications: Multitaper and Conventional Univariate Techniques*, Cambridge University Press, New York.

Primak, S. and Sejdić, E. (2008). Application of multitaper analysis to wireless communications problems, *Proc. of First International Symposium on Applied Sciences on Biomedical and Communication Technologies (ISABEL 2008)*, Aalborg, Denmark.

Proakis, J. (2001). *Digital Communications*, fourth edn, McGraw-Hill, New York.

Rao, A. and Hamed, K. (2003). Multi-taper method of analysis of periodicities in hydrologic data, *Journal of Hydrology* **279**: 125–143.

Rappaport, T. (2002). *Wireless Communications: Principles and practice*, Prentice Hall, Upper Saddle River.

Salz, J. and Winters, J. (1994). Effect of fading correlation on adaptive arrays in digital mobile radio, *IEEE Trans. Veh. Technol.* **43**(4): 1049–1057.

Schreier, P. and Scharf, L. (2003). Second-order analysis of improper complex random vectors and processes, *IEEE Trans. Signal Process.* **51**(3): 714–725.

SCM Editors (2006). UMTS: Spatial channel model for MIMO simulations, *Tech. report 25.996*.

Sejdić, E., Luccini, M., Primak, S., Baddour, K. and Willink, T. (2008). Channel estimation

using DPSS based frames, *Proc. of IEEE International Conf. on Acoustics, Speech, and Signal Processing (ICASSP 2008)*, Las Vegas, USA, pp. 2849–2852.

Sen, I. and Matolak, D. (2008). Vehiclevehicle channel models for the 5-GHz band, *IEEE Trans. Intell. Transp. Syst.* **9**(26): 235–245.

Simon, M. and Alouini, M.-S. (2000). *Digital Communication over Fading Channels:A Unified Approach to Performance Analysis*, John Wiley & Sons, New York.

Slepian, D. (1978). Prolate spheroidal wave functions, Fourier analysis, and uncertainty. V-The discrete case, *Bell System Technical Journal* **57**: 1371–1430.

Stoica, P. and Sundin, T. (1999). On nonparametric spectral estimation, *Journal of Circuits, Systems, and Signal Processing* **18**(2): 169–181.

Thomson, D. (1998). Multiple-window spectrum estimates for non-stationary data, *Proc. of Ninth IEEE SP Workshop on Statistical Signal and Array Processing, 1998*, pp. 344–347.

Thomson, D. (2000). Multitaper Analysis of Nonstationary and Nonlinear Time Series Data, *Nonlinear and Nonstationary Signal Processing* .

Thomson, D. J. (1982). Spectrum estimation and harmonic analysis, *Proceedings of the IEEE* **70**(9): 1055–1096.

van Trees, H. (2001). *Detection, Estimation, and Moduclation Theory: Part I*, first edn, John Wiley & Sons, New York.

van Trees, H. (2002). *Detection, Estimation and Modulation Theory: Optimal Array Processing*, first edn, Wiley-Interscience, New York.

Xiao, H., Burr, A. and White, G. (2005). Simulation of time-selective environment by 3GPP spatial channel model and analysis on the performance evaluation by the CMD metric, *Proc. International Wireless Summit (IWS 05)*, Aalborg, Denmark, pp. 446–450.

Yip, K. and Ng, T. (1997). Karhunen-Loeve expansion of the WSSUS channel output and its application to efficient simulation, *IEEE J. Sel. Areas Commun.* **15**(4): 640–646.

Zemen, T., Hofstetter, H. and Steinbck, G. (2005). Slepian subspace projection in time and frequency for time-variant channel estimation, *14th IST Mobile and Wireless Summit*, Dresden, Germany.

Zemen, T. and Mecklenbräuker, C. F. (2005). Time-variant channel estimation using discrete prolate spheroidal sequences, *IEEE Transactions on Signal Processing* **53**(9): 3597–3607.

Zemen, T., Mecklenbräuker, C. F. and Fleury, B. (2006). Time-variant channel prediction using time-concentrated and band-limited sequences, *Proc. of 2006 IEEE International Conference on Communications (ICC '06)*, Vol. 12, Istanbul, Turkey, pp. 5660–5665.